



ELSEVIER

Contents lists available at ScienceDirect

Mechatronics

journal homepage: www.elsevier.com/locate/mechatronics

Modeling and compensation of asymmetric hysteresis for pneumatic artificial muscles with a modified generalized Prandtl–Ishlinskii model[☆]

Sheng-Long Xie^a, Hai-Tao Liu^{a,*}, Jiang-Ping Mei^a, Guo-Ying Gu^b^a Key Laboratory of Mechanism Theory and Equipment Design, Ministry of Education, Tianjin University, Tianjin 300072, PR China^b State Key Laboratory of Mechanical System and Vibration, Shanghai Jiao Tong University, Shanghai 200240, PR China

ARTICLE INFO

Keywords:

Asymmetric hysteresis modeling
Inverse hysteresis compensation
Pneumatic artificial muscle (PAM)
Modified generalized Prandtl–Ishlinskii (MGPI) model

ABSTRACT

This paper presents a modified generalized Prandtl–Ishlinskii (MGPI) model for the asymmetric hysteresis characterization of pneumatic artificial muscles (PAMs), which can be considered as a cascade of the superposition of weighted generalized play operators and the superposition of weighted dead-zone operators. Compared with the established hysteresis models, the significance of the MGPI model is that it has a simple expression including a small number of parameters to be identified. Besides, the analytical form of its inverse model is easy to be obtained, which can be applied to the compensation of asymmetric hysteresis of the PAM in real-time. The wiping-out and congruency properties of the proposed model are verified by simulations. Meanwhile, by carrying out the experimental study on length–pressure hysteresis of a PAM, the parameters in the MGPI model are identified from measured data using the Levenberg–Marquardt method. Then, a feedforward hysteresis compensator based on the inverse MGPI model is designed for trajectory tracking control of the PAM. The simulation and experimental results indicate that the proposed model and its inversion are effective to characterize and compensate the length–pressure hysteresis of the PAM.

1. Introduction

Hysteresis is a common nonlinear phenomenon that appears in various systems, including smart materials [1], ferromagnetic materials [2] and pneumatic artificial muscles (PAMs) [3]. The hysteresis properties can cause inaccuracies and oscillations in the system responses [4], yielding degraded performance of the system. Significant efforts have been made toward the modeling of hysteresis properties for effective controller designs.

The existing models characterized the hysteresis can be classified into physics-based models and phenomenology-based models. The physics-based models [5] are usually derived on the basis of physical principles of the particular material and/or system properties. In contrast, the phenomenological hysteresis models are constructed based on the experimental data without considering the physical properties of the actuator, and thus have been adopted more extensively. The phenomenology-based models can be roughly divided into two classes [6]: (1) operator-based models, which utilizes different kinds of mathematical operators to characterize the hysteresis loops, such as Preisach model [7], Krasnosel'skii–Pokrovskii (KP) model [8], Prandtl–Ishlinskii (PI) model [9], Maxwell-slip model [10] and its modified version [11];

(2) differential-based models, which adopts nonlinear differential equations to characterize hysteresis dynamics [12], such as Dahl model [13], LuGre model [14], Duhem model [15,16], Bouc–Wen model [17] and its variations [18].

As a subclass of the Preisach model, the PI model [19], which is a linearly weighted superposition of elementary linear play operators with different thresholds and weighting values, is the most widely used model in both hysteresis modeling and control. Compared with other models, the main advantage of the PI model lies in its simple expression and analytical inversion, thus making it more efficient for real-time applications. However, the classical PI (CPI) model is not adequate to describe the nonlinear and saturated hysteresis loops [20] because the linear play operator is symmetric and convex. In an attempt to overcome these drawbacks of the CPI model, a lot of variations of the PI model have been proposed by: (1) cascading linear play operators with continuous non-convex and asymmetric memory-free superposition operators in series [21]; (2) replacing the linear play operators with nonlinear ones; and (3) adding nonlinear memoryless function [22] (or nonlinear input function [23]). Kuhnen [21] proposed a modified PI (MPI) model that combines linear play operators with one-sided dead-zone operators (DZOs) to model the asymmetric hysteresis. Along this

[☆] This paper was recommended for publication by Associate Editor Dr Wei-Hsin Liao.

* Corresponding author.

E-mail address: liuht@tju.edu.cn (H.-T. Liu).

track, Wei et al. [24] developed a rate-dependent MPI model to take account of the hysteretic nonlinearity of a piezoelectric actuator at varying frequency. Al Janaideh et al. [25] applied a symmetric generalized PI (SGPI) model to characterize the symmetric and saturated hysteresis loops. To improve the capability of the SGPI model in capturing the asymmetric hysteresis loops, an enhanced SGPI, named asymmetric GPI (AGPI) model, was proposed by adopting different envelope functions under increasing and decreasing inputs, which is more effective in describing the complex asymmetric hysteresis with output saturation compared to the SGPI model [26]. Subsequently, the analytical inversion of the AGPI model was further derived in [27]. Meanwhile, based on the CPI model, Jiang et al. [28] modeled the hysteresis nonlinearity of piezoelectric actuators by proposing two asymmetric operators to describe the ascending and descending branches of the hysteresis independently. The AGPI model [27] can capture asymmetric hysteresis with output saturation, and it has an analytical inversion as long as the envelope functions of all the generalized play operators are in the same form [22]. However, the same form of envelope functions in AGPI model limits its modeling capability [29]. Hence, Zhang et al. [22] formulated an extended generalized PI (EGPI) model by adding a nonlinear memoryless function into the AGPI model, and presented an iterative inversion algorithm based on the Fixed-Point Theorem to derive its inversion. The result indicates that the EGPI model has better capability to describe complex hysteresis than the AGPI model. Moreover, Gu et al. [30] combined a CPI model with a nonlinear non-hysteretic function of the input to capture the asymmetric hysteresis of piezoceramic actuators. However, the proposed model is not suitable for PAMs due to the convexity property [21] of the PI model.

In this paper, a novel modified generalized PI (MGPI) model combining the SGPI with MPI models is formulated to identify the asymmetric hysteresis of PAMs. The main advantages of the proposed MGPI model lie in that: (1) rather than the different envelope functions used in AGPI and EGPI models, the hysteresis envelope functions of this model are the same as those of the SGPI model, thus it has a simple mathematical expression to describe the asymmetric hysteresis behavior of PAMs; (2) due to (1), the MGPI model has a relative fewer parameters to be identified compared with MPI model; (3) the analytical inverse of the MGPI model can be directly derived from that of the SGPI and MPI models. To validate the developed model and the inverse hysteresis compensator, the results of simulation and experiment on a PAM are presented.

The rest of this paper is organized as follows. Section 2 presents the MGPI model and its analytical inversion. The verification of wiping-out and congruency properties of the developed MGPI model is given in Section 3. Finally, an inverse-based hysteresis compensator for trajectory tracking control of the PAM is designed in Section 4 to validate the capacity of the proposed model before conclusions are drawn in Section 5.

2. MGPI model

The analytical formulations of the MGPI model and its inverse model are presented in this section. The former is used to characterize the asymmetric length–pressure hysteresis, while the latter is applied as a feedforward compensator for trajectory tracking control.

2.1. AGPI model

The AGPI model [26,27] is an operator-based phenomenological model, which utilizes the weighted generalized play operators (GPOs) to describe the nonlinear and saturated hysteresis nonlinearity. The input–output relationship of a GPO is shown in Fig. 1, which is characterized by the input x and the thresholds ζ_r and ζ_l . The increase of input x causes the output w increasing along the curve γ_r , while the decrease of x causes w decreasing along the curve γ_l , resulting in a

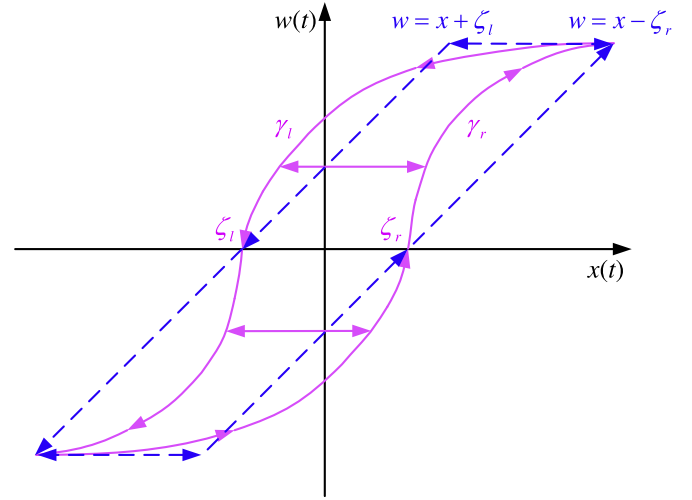


Fig. 1. Input–output relationship of the generalized play operator.

asymmetric hysteresis loop. The curves γ_l and γ_r are the envelop functions of GPO, which are strictly continuous and increasing, satisfying $\gamma_l \geq \gamma_r$ [25].

Suppose that $C_m[0, T]$ is the space of piecewise monotone continuous functions. According to the definition presented in [31], the output of the GPO, denoted by F_r^y , for any input $x(t) \in C_m[0, T]$ can be formulated as

$$\begin{aligned} w(0) &= F_r^y[x](0) = f_r^y(x(0), 0) \\ w(t) &= F_r^y[x](t) = f_r^y(x(t), F_r^y[x](t_i)) \end{aligned} \quad (1)$$

for $t_i < t < t_{i+1}$ and $0 \leq i \leq N - 1$, with

$$f_r^y(x, w) = \max(\gamma_r(x) - r, \min(\gamma_l(x) + r, w)) \quad (2)$$

where $0 = t_0 < t_1 < \dots < t_N = T$ are intervals in $C_m[0, T]$ such that the input function $x(t)$ is monotone on each of the subintervals $[t_i, t_{i+1}]$. r is the threshold value of the GPO, which is defined as

$$r = \frac{\gamma_r(\zeta_r) - \gamma_l(\zeta_l)}{2} \quad (3)$$

The AGPI model can be subsequently formulated by integrating the GPO and the density function $p(r)$, yielding

$$y_p(t) = H(x(t)) + \int_0^T p(r) F_r^y[x](t) dr \quad (4)$$

where $p(r)$ is an integrable positive density function; H is the non-decreasing Lipschitz continuous function.

$$H(x(t)) = \begin{cases} q\gamma_r(x(t)) & \text{if } \dot{x} \geq 0 \\ q\gamma_l(x(t)) & \text{if } \dot{x} < 0 \end{cases} \quad (5)$$

To implement the real-time control, the AGPI model (4) can also be approximately expressed in the form of a finite number of the GPOs [26], resulting in

$$y_p(k) = F_r^y[x(k), \mathbf{y}_0] = q\gamma(x(k)) + \sum_{i=1}^n p_i(r_i) F_{r_i}^y[x](k) \quad (6)$$

$$F_{r_i}^y[x](k) = \max(\gamma_r(x) - r_i, \min(\gamma_l(x) + r_i, F_{r_i}^y[x](k-1))) \quad (7)$$

$$\gamma(x(k)) = \begin{cases} \gamma_r(x(k)) & \text{if } \dot{x} \geq 0 \\ \gamma_l(x(k)) & \text{if } \dot{x} < 0 \end{cases} \quad (8)$$

where n is the number of GPOs; q is a positive constant; $\mathbf{y}_0 = [y_{10}, \dots, y_{n0}]^T$ is the initial state. The threshold value r_i and the weight of the i th operator p_i can be given as

$$r_i = \alpha i \quad (9)$$

$$p_i = p(r_i) = \rho e^{-\tau r_i} \quad (10)$$

where α , ρ and τ are positive constants identified from experimental data of the PAM.

Remark. The AGPI model [26] utilizes different nonlinear envelope functions to approach the asymmetric hysteresis loops, i.e. $\gamma_l(x) \neq \gamma_r(x)$, for the ascending and descending branches. Therefore, it can characterize the asymmetric and saturated hysteresis loops. As a special case of the AGPI model, the SGPI model [25] employs the same envelope functions, i.e. $\gamma_l(x) = \gamma_r(x) = \gamma$. Although it has limitation on describing the asymmetric hysteresis [25], the formulation of this model is simple.

2.2. MGPI model

Taking advantage of the SGPI model and the MPI model, a novel MGPI model is proposed in this paper for the description of the asymmetric hysteresis behavior of PAMs. The SGPI model is utilized to reduce the complexity of modeling, while the capability of characterizing the asymmetric hysteresis is enhanced by cascading the one-side dead-zone operators.

According to [25], the envelop function is given by

$$\gamma(x(t)) = c_0 \tanh[c_1 x(t) + c_2] + c_3 \quad (11)$$

where $c_0 > 0$, $c_1 > 0$, c_2 , c_3 are constants to be identified. Then, the proposed MGPI model can be derived as the cascade of superposition of weighted GPOs and superposition of weighted dead-zone operators (DZOs). For different threshold values, Fig. 2 shows the input–output relationship of the DZOs, which can be defined as [21]

$$z(t) = S_d[y](t) = S(y(t), d) \quad (12)$$

$$S(y(t), d) = \begin{cases} \max\{y(t) - d, 0\} & d > 0 \\ y(t) & d = 0 \\ \min\{y(t) - d, 0\} & d < 0 \end{cases} \quad (13)$$

Thus, the output of dead-zone (DZ) model can be expressed as follows

$$y_s(k) = \mathbf{w}_s^T \mathbf{S}_d[y](k) \quad (14)$$

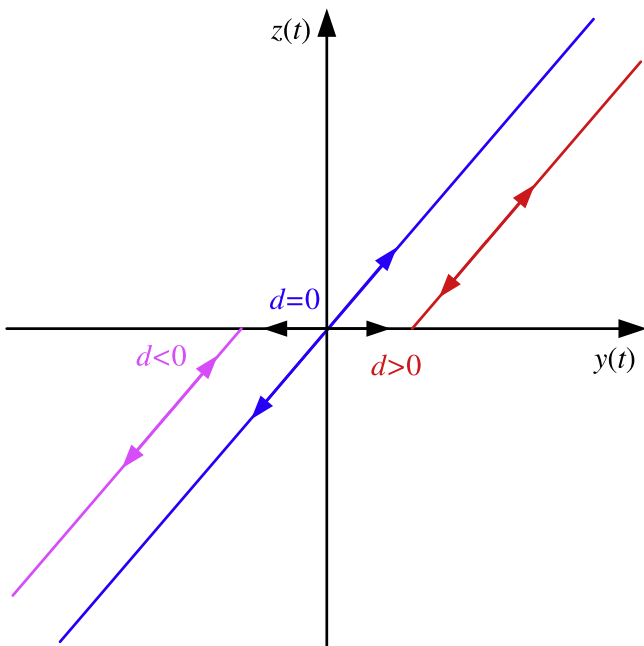


Fig. 2. Input–output relationship of the dead-zone operator.

$$\mathbf{w}_s = (w_{s0}, w_{s1}, \dots, w_{sm})^T, \quad \mathbf{d} = (d_0, d_1, \dots, d_m)^T$$

$$\mathbf{S}_d[y](k) = (S_{d0}[y](k), S_{d1}[y](k), \dots, S_{dm}[y](k))^T$$

where $y_s(k)$ is the output of DZ model; \mathbf{w}_s , $\mathbf{S}_d[y](k)$ and \mathbf{d} are the vectors of weights, DZOs and thresholds, respectively. The element in \mathbf{d} is defined as

$$d_j = \frac{j}{m} \max(y_p) \quad (15)$$

Thus, by using a finite number of the GPOs and DZOs, the MGPI model can be derived

$$y_M(k) = \Gamma[x](k) = \mathbf{w}_s^T \mathbf{S}_d[\mathbf{F}_r^T[x(k), \mathbf{y}_0]] \quad (16)$$

It is notable that the MGPI model is different from the variations of the CPI models [19], such as the AGPI model and EGPI model. To overcome the drawback of the CPI model that can only describe the symmetric hysteresis, the AGPI model proposed in [26] and [27] modified the GPOs by using two different envelope functions. While the EGPI models developed in [22] and [29] replaced the function $H(x(t))$ by a new nonlinear function. By contrast, the MGPI model combines the GPOs of the SGPI model with the superposition of dead-zone operators (Fig. 3). In this manner, the developed model has a simple mathematical expression using fewer parameters to characterize the asymmetric hysteresis behavior. Another advantage is that the analytical inversion of the MGPI model can be directly derived from that of the CGPI model and MPI model for the real-time feedforward hysteresis compensation, which will be investigated in Section 4.

2.3. Inverse MGPI model

Referring to [21,25], the inverse MGPI model can be obtained from that of the SGPI model and MPI model, which can be formulated as

$$x(k) = \Gamma^{-1}[y](k) = y_p'[\mathbf{w}_p^T \mathbf{S}'_d[y]](k) \quad (17)$$

where

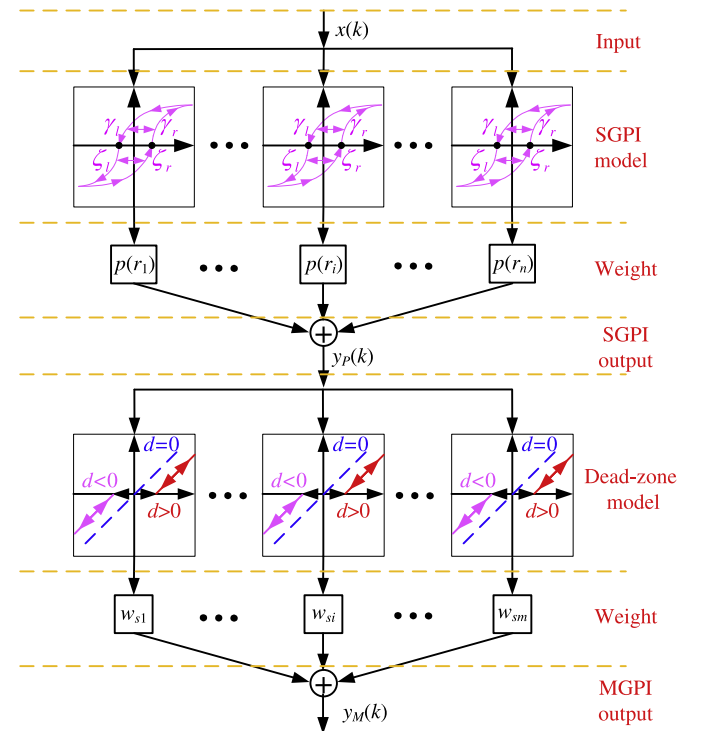


Fig. 3. Structure of MGPI model.

$$y_p'(k) = \gamma^{-1} \left(q'y(k) + \sum_{i=1}^n p'_i x_i(k) \right) \quad (18)$$

$$x_i(k) = \max\{y(k) - r'_i, \min\{y(k) + r'_i, x_i(k-1)\}\} \quad (19)$$

$$\begin{cases} w'_{s0} = \frac{1}{w_{s0}} \\ w'_{sj} = \frac{-w_{sj}}{(\sum_{k=0}^j w_{sk})(\sum_{k=0}^{j-1} w_{sk})} \\ d'_j = \sum_{k=0}^j w_{sk}(d_j - d_k) \end{cases} \quad (20)$$

$$\begin{cases} q' = \frac{1}{q} \\ r'_i = qr_i + \sum_{j=1}^{i-1} p_j(r_i - r_j) \\ p'_i = \frac{-p_i}{\left(q + \sum_{j=1}^i p_j\right) \left(q + \sum_{j=1}^{i-1} p_j\right)} \end{cases} \quad (21)$$

Here, $x_i(k)$ is the i th inverse generalized linear play operator; r'_i and p'_i are the threshold and weight of the inverse GPI model, respectively.

3. Verification of wiping-out and congruency properties

Although the MPI model can capture the asymmetric hysteresis loops, the wiping-out and congruency properties of this model are not verified in [21]. Since these two properties are essential for validating the effectiveness of operator-based hysteresis models [32], the corresponding simulations on the proposed MGPI model are carried out in this section.

3.1. Wiping-out property

The wiping-out property means that the output of hysteresis loops depends on not only the current input but also the alternating series of previous dominant input extrema. As a nonlocal memoryless behavior of the hysteresis, only the alternating series of previous dominant input extrema are stored, and the memories of all the other inputs are wiped out.

Fig. 4(a) illustrates the input pressure signal, which is given to verify the wiping-out property. There are two local minimal values (p_2

and p_4), two local maximal values (p_1 and p_3) and one global maximal value (p_5). Fig. 4(b) shows the hysteresis loops generated by the given input pressure. When the input signal decreases from p_3 to p_4 , the hysteresis loop moves from point L_3 to point L_4 . Since the value p_4 is smaller than that of p_2 , the memory point L_2 is wiped out by the memory point L_4 . When the input increases from p_4 to p_5 , due to $p_5 > p_1 > p_3$, the memory points L_1 and L_3 are both wiped out by the new memory point L_5 . The simulation results indicate that the MGPI model successfully fulfills the wiping-out property.

3.2. Congruency property

The congruency property refers to the characteristic that two minor hysteresis loops with the same input range are congruent. It means that one minor loop can overlap the other by pure translation.

The input pressure signal for the validation of congruency property is shown in Fig. 5(a). There are two local minimal values (p_2 and p_4) and two local maximal values (p_1 and p_3), satisfying $p_5 = p_1$ and $p_2 = p_4$. Thus, we have $[p_2, p_1] = [p_4, p_3]$. Fig. 5(b) is the corresponding hysteresis loops. There are two minor hysteresis loops, namely, loop 1 and loop 2. The lower minor hysteresis loop 1 is obtained from the input pressure between p_1 to p_2 in the ascending branch, and the upper loop 2 is caused by the input pressure between p_4 to p_5 in the descending branch. Obviously, these two minor loops can overlap each other exactly after shifting a distance, which demonstrates that the two minor loops are congruent.

4. Experimental verification

In this section, the experiment on the length–pressure hysteresis of a PAM is conducted. By using the Levenberg–Marquardt method, the parameters in the MGPI model are identified from the experimental data. Then, an inverse-based compensator for trajectory tracking control of the PAM is designed to demonstrate the effectiveness of the model.

4.1. Experimental apparatus

The experimental apparatus is shown in Fig. 6, which consists of a PAM, a VPPM valve, an air compressor, a displacement sensor, a pressure sensor and a computer. The PAM is DMSP-20-500 N fluidic muscle (internal diameter: 20 mm; length: 500 mm) manufactured by Festo, of which one extremity is connected with the base and the other moves freely. The length and the internal pressure of the PAM are

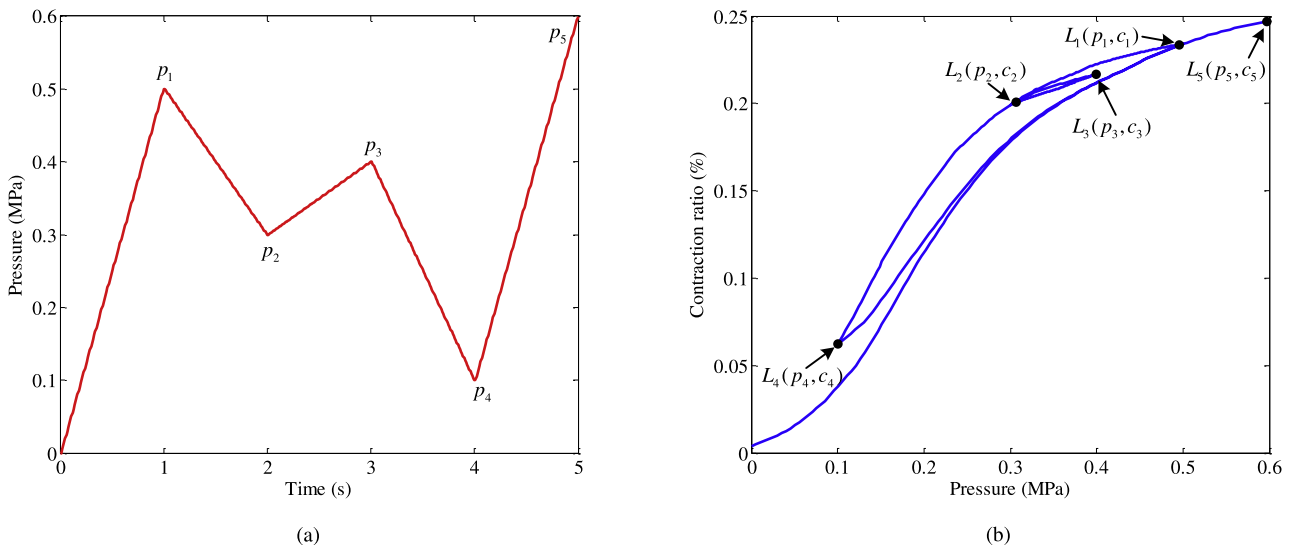
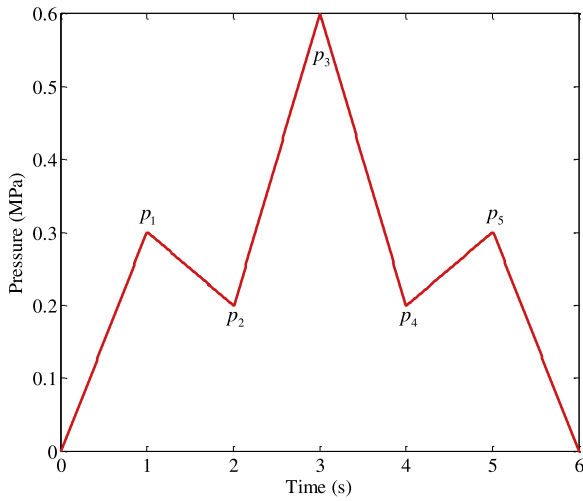
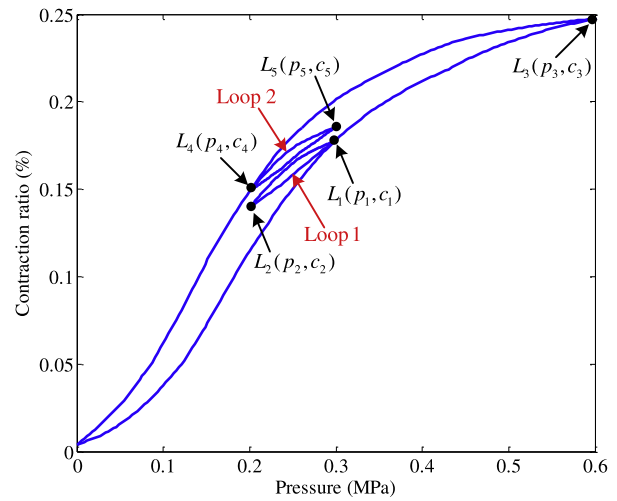


Fig. 4. Simulation of the wiping-out property. (a) Input pressure. (b) Hysteresis loops.



(a)



(b)

Fig. 5. Simulation of the congruency property. (a) Input pressure. (b) Hysteresis loops.

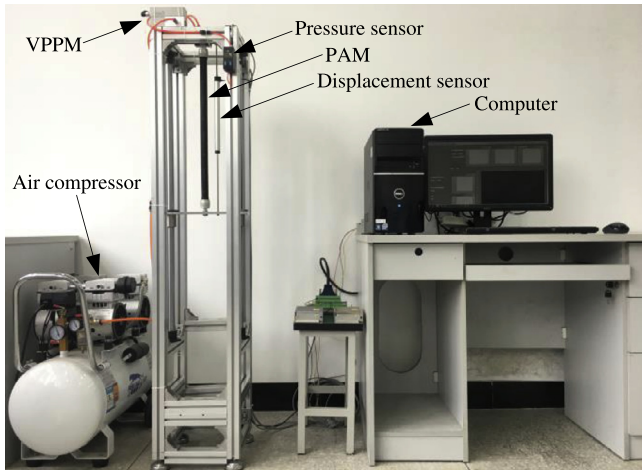


Fig. 6. Experimental apparatus.

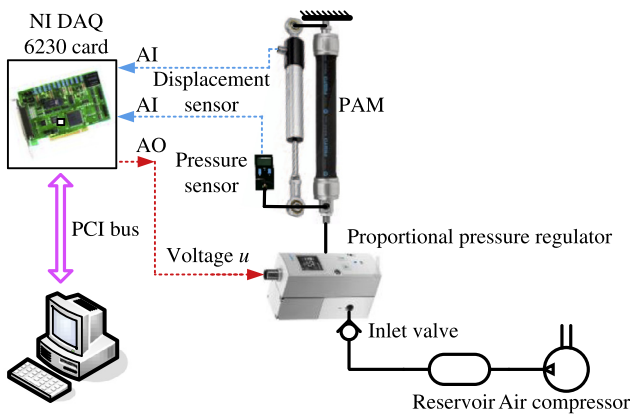


Fig. 7. Schematic diagram of the experimental setup.

measured by a displacement sensor (Novotechnik TEX-0150) and a pressure transducer (FESTO SDE1-D10), respectively. A proportional pressure regulator (Festo VPPM-6L-L-1-G18-0L10H) is equipped to regulate the required pressure for the PAM. Fig. 7 shows the schematic diagram of the experimental setup, where a NI data acquisition board 6230 is embedded in the computer and the control algorithm are developed using the graphical programming platform of LabVIEW.

Table 1

Identified parameters of the GPI model.

c_0	c_1	c_2	c_3
1.6867	0.3385	-0.2319	0.3211
Q	ρ	τ	α
0.2959	0.1827	5.4999	0.08

Table 2

Identified parameters of the DZ model.

Number	w_i	Number	w_i
1	0.1207	6	-0.0238
2	0.0246	7	-0.0070
3	0.0405	8	-0.0401
4	0.0694	9	-0.0223
5	0.0357	10	0.0625

Table 3

Comparison of different models with different n .

n	Models	ME/mm	MAE/mm	RMSE/mm
10	MGPI	3.0506	0.6116	0.8518
	SGPI	5.2507	1.0725	1.3726
20	MGPI	2.9791	0.5798	0.8061
	SGPI	5.3458	1.061	1.3636

Table 4

Comparison of MGPI model with different m .

m	ME/mm	MAE/mm	RMSE/mm
10	3.0506	0.6116	0.8518
14	3.4331	0.5828	0.8136

4.2. Hysteresis loops characterization

Before the experimental verification of the proposed MGPI model, the parameters identification is necessary. However, parameters identification of the MGPI model is by no means an easy task, due to the high-dimensional, high-nonlinear and multi-constraint characteristics. There are many algorithms having been developed to solve the problem of parameter identification of hysteresis models, such as the particle swarm optimization [33], genetic algorithm [34], covariance matrix

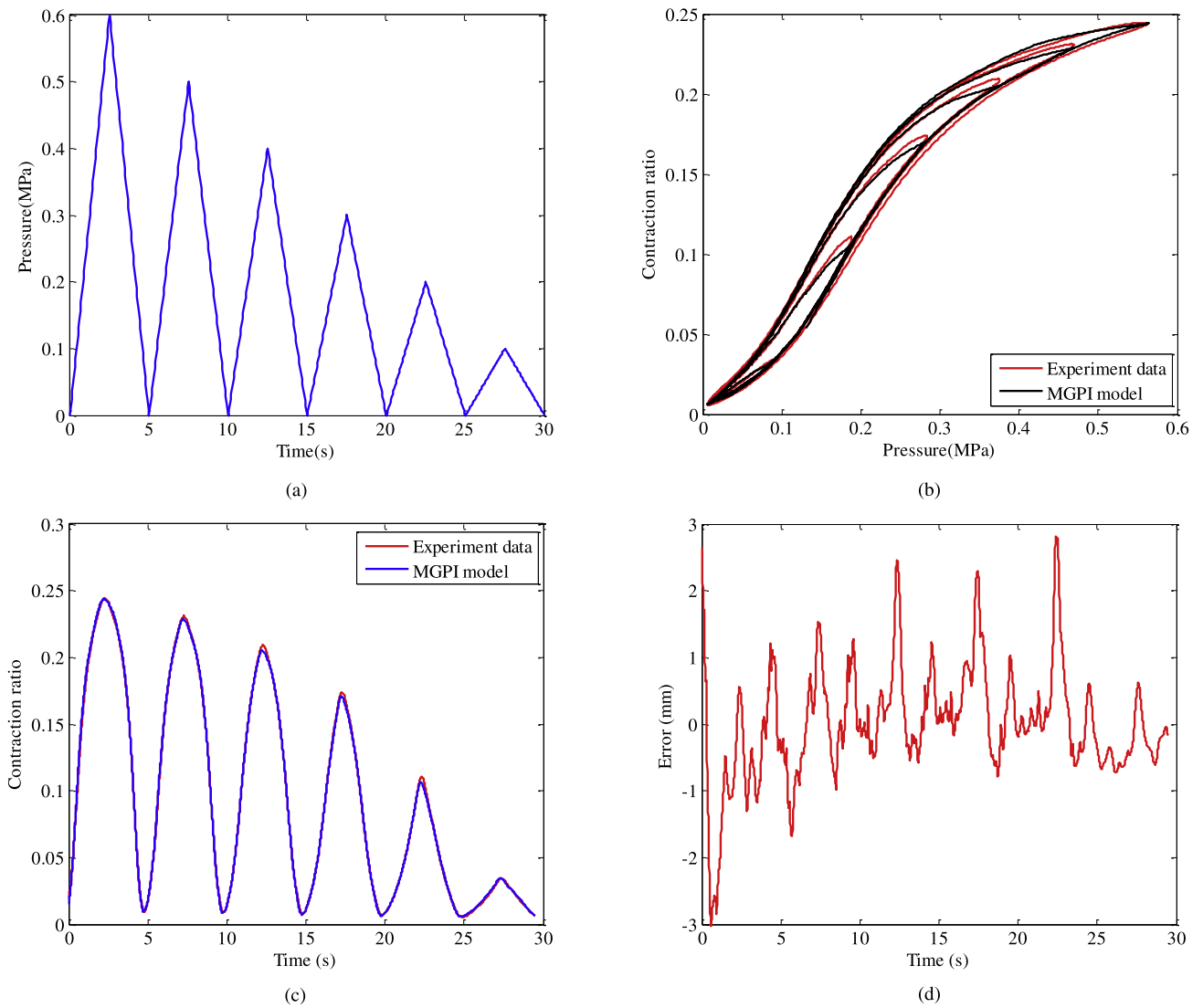


Fig. 8. Experimental verification of the MGPI model. (a) Input pressure. (b) Hysteresis loops. (c) Length of PAM. (d) Error.

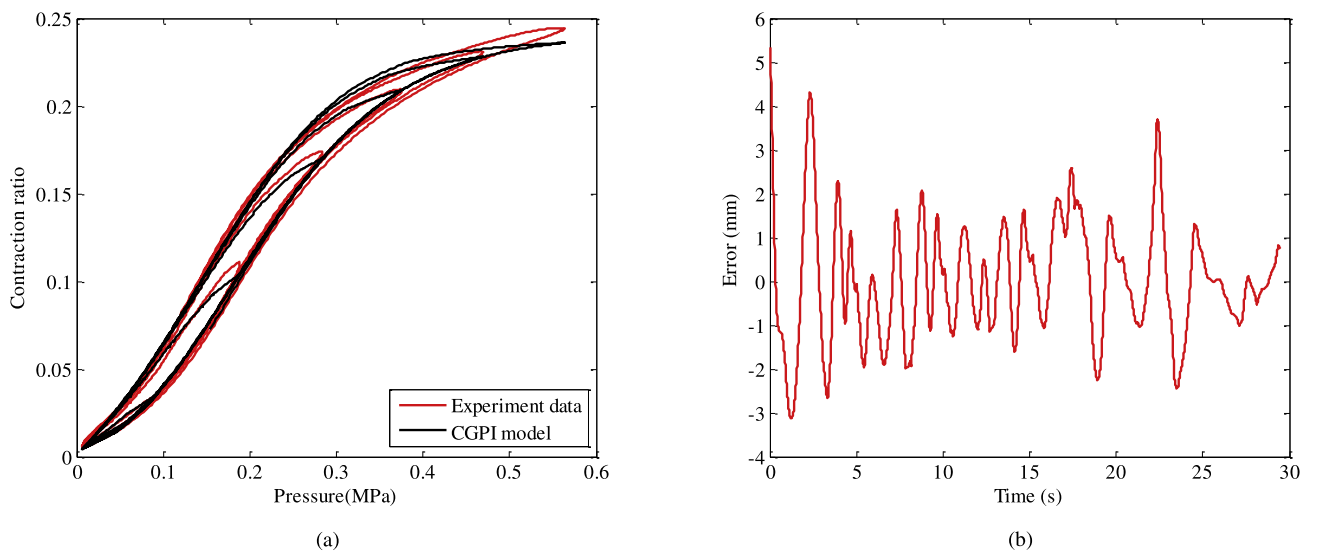


Fig. 9. Experimental verification of the AGPI model. (a) Hysteresis loops. (b) Error.

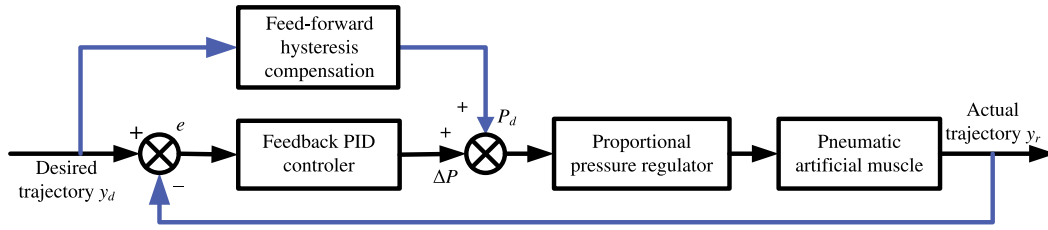


Fig. 10. Block diagram of the controlled system.

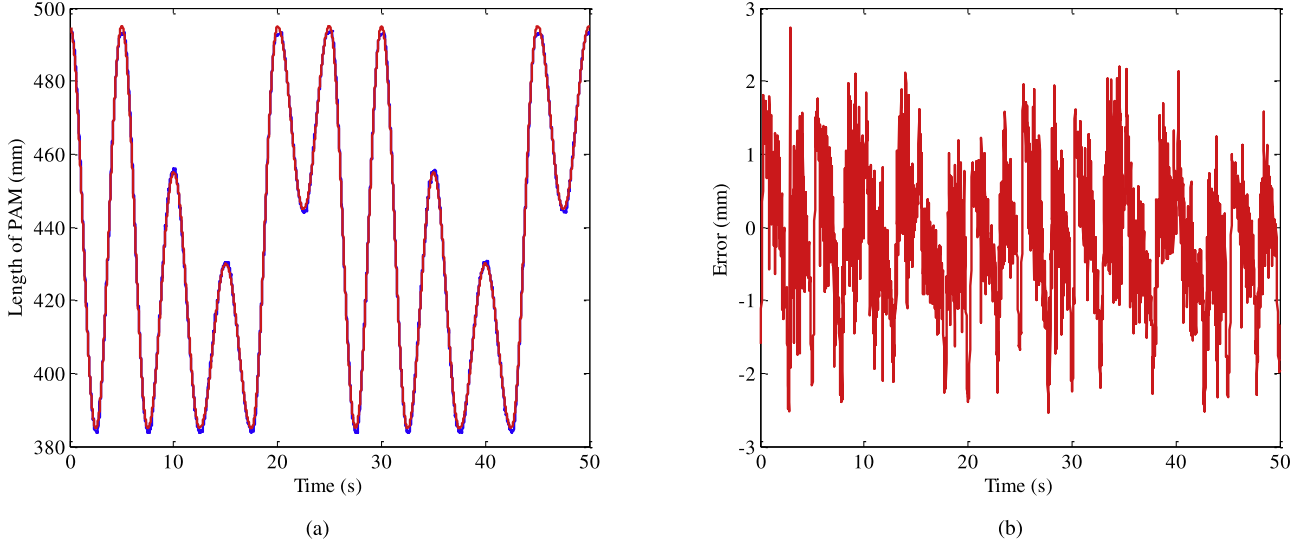


Fig. 11. Demonstration of the inverse hysteresis compensation performance. (a) Trajectory tracking response. (b) Error.

adaptation evolution strategy [35]. In this paper, the Levenberg–Marquardt method [36] is adopted to identify the parameters in the MGPI model by minimizing the following quadratic cost function.

$$J(\boldsymbol{\theta}) = \mathbf{E}^T(\boldsymbol{\theta})\mathbf{E}(\boldsymbol{\theta}) = \sum_{k=1}^N (y(k) - y_M(k, \boldsymbol{\theta}))^2 \quad (22)$$

subject to

$$\begin{cases} y_M(k, \boldsymbol{\theta}) = \mathbf{w}_s^T \mathbf{S}_d [F_r^y [x(k), y_0]] \\ \boldsymbol{\theta} = [\boldsymbol{\theta}_g; \boldsymbol{\theta}_d] \\ \boldsymbol{\theta}_g = [c_0, c_1, c_2, c_3, q, \rho, \tau, \alpha]^T \\ \boldsymbol{\theta}_d = [w_{s1}, \dots, w_{sm}]^T \\ c_0 > 0, c_1 > 0, \rho > 0, \tau > 0, \alpha > 0 \end{cases} \quad (23)$$

where $\boldsymbol{\theta} = [\boldsymbol{\theta}_g; \boldsymbol{\theta}_d]$ is the vector of parameters to be identified; $\boldsymbol{\theta}_g$ and $\boldsymbol{\theta}_d$ are the parameters in the GPI model and DZ model, respectively; x and y are input and output data obtained from the experiment; N is the number of x ; $\mathbf{E}(\boldsymbol{\theta})$ is the error vector; y_M is the output of the MGPI model.

The identified parameters of the MGPI model (16) using ten GPOs ($n = 10$) and ten DZOs ($m = 10$) are summarized in Tables 1 and 2. It should be pointed out that the larger the numbers of n and m , the higher the precision of the MGPI model to capture the hysteresis loops. However, it is found that further increase of the numbers of GPOs and DZOs does not improve the modeling accuracy significantly, which can be seen from Tables 3 and 4. These conclusions are consistent with the results obtained in [21] and [30].

By using the identified parameters, it is easy to carry out the comparison study between the experimental data of length–pressure hysteresis loops of the PAM and the prediction results of the MGPI model. The reference pressure signal is designed in the form of triangle-wave as shown in Fig. 8(a). Its amplitude decreases from 0.6 MPa to 0.1 MPa with an equal interval of 0.1 MPa. Fig. 8(b) illustrates the

length–pressure hysteresis loops obtained from the MGPI model and experimental data. It can be seen that the proposed model is very effective in characterizing both major and minor hysteresis loops of the PAM. Fig. 8(c) shows that the prediction results of the MGPI model match the experimental measurements very well. The maximal error is 3.0506 mm in the full range of movement (see Fig. 8(d) and Table 3).

To demonstrate the advantage of the proposed MGPI model, the SGPI model is also developed to describe the length–pressure hysteresis of the PAM under the same input pressure signal, resulting in the hysteresis loops depicted in Fig. 9. It can be seen that the error of the SGPI model is larger than that of the MGPI model, indicating that the proposed model has a better capability of characterizing the asymmetric length–pressure hysteresis behavior of PAMs.

4.3. Hysteresis nonlinearity compensation

To compensate the length–pressure hysteresis, a feedforward and feedback combined control strategy is proposed to realize high accurate trajectory tracking control of the PAM. Given the identified parameters of the MGPI model, the inverse MGPI model can be obtained using (17)–(21), which can be cascaded with the control system as a feedforward hysteresis compensator. The inverse MGPI model maps the desired trajectory y_d into an actual control input P_d applied on the proportional pressure regulator. Hence, the relationship between the desired trajectory y_d and actual length y_r can be linearized. Note that the accuracy of the hysteresis model affects the performance of the feedforward controller. Therefore, a feedback loop has to be added to form a feedforward and feedback combined controller. The control scheme is illustrated in Fig. 10. A conventional PID controller is placed in the feedback loop, which has the form

$$\Delta P = K_p e(t) + K_i \int_0^t e(\tau) d\tau + K_d \frac{de(t)}{dt} \quad (24)$$

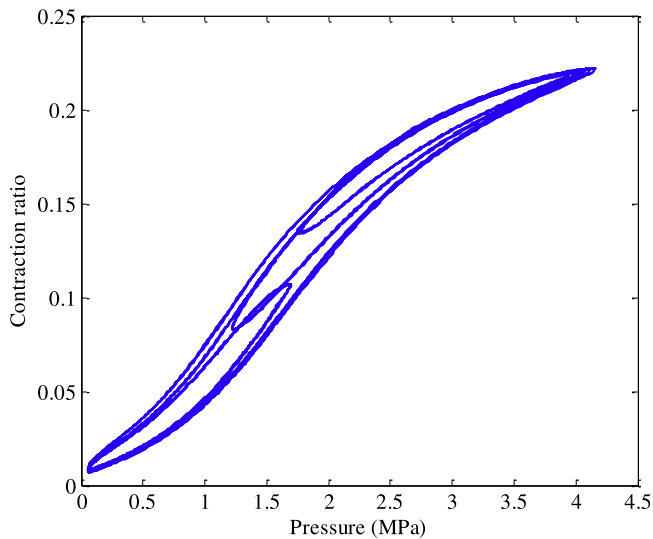


Fig. 12. Demonstration of the length–pressure hysteresis loops of PAM.

Table 5
Trajectory tracking errors.

ME/mm	MAE/mm	RMSE/mm
2.738	0.7153	0.8975

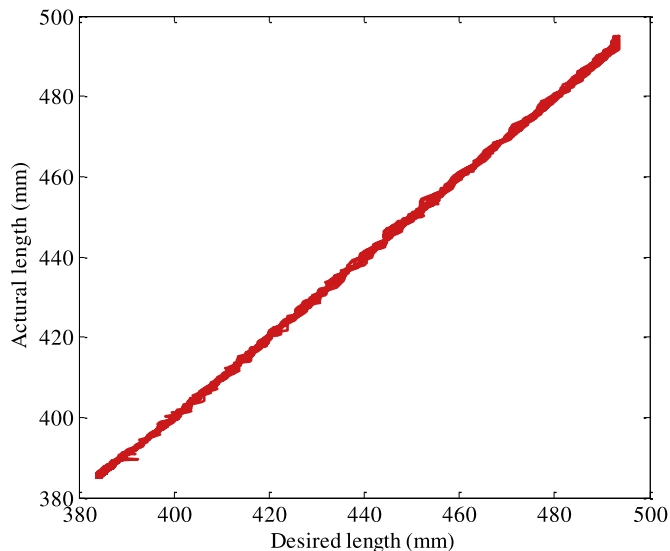


Fig. 13. Relationship between the desired length and the actual length after compensation.

where $e(t)$ is the tracking error signal; ΔP is output of PID controller; K_p , K_i and K_d are proportional, integral and derivative gains, respectively, which are given as $K_p = 0.05$, $K_i = 0.01$ and $K_p = 0$.

The tracking responses and errors of the proposed control scheme are shown in Fig. 11. The corresponding length–pressure hysteresis loops of the PAM are demonstrated in Fig. 12. Table 5 lists the statistics of the trajectory tracking error. It can be found that the maximal error is 2.738 mm, and the mean absolute error is only 0.7153 mm. The experimental results show that the inverse MGPI model is effective to compensate for the asymmetric length–pressure hysteresis in real-time application. This conclusion can also be drawn from the nearly linear relationship between the desired and the actual lengths of the PAM after compensation, as shown in Fig. 13.

5. Conclusion

To precisely characterize the asymmetric hysteresis nonlinearity of the PAM, a MGPI model is proposed in this paper. The following conclusions are drawn.

- (1) The proposed MGPI model can be considered as a cascade of the superposition of weighted generalized play operators and the superposition of weighted dead-zone operators. Referring to the inversions of the SGPI and MPI models, the analytical form of the inverse MGPI model can be easily derived, which is readily available for hysteresis compensation.
- (2) The wiping-out and congruency properties of the proposed model are testified by simulations. The results show that the MGPI model successfully fulfills both properties.
- (3) The results of experimental verification indicate that the MGPI model has a better capability of describing the length–pressure hysteresis of PAMs compared with the SGPI model, and its inversion is effective for the compensation of the asymmetric hysteresis.

Acknowledgments

This work was supported by National Natural Science Foundation of China under grant 51405331.

References

- [1] Song G, Zhao J, Zhou X, et al. Tracking control of a piezoceramic actuator with hysteresis compensation using inverse Preisach model. *IEEE/ASME Trans Mechatron* 2005;10(2):198–209.
- [2] Tan XB, Baras JS. Modeling and control of hysteresis in magnetostrictive actuators. *IEEE Control Syst* 2004;40(9):1469–80.
- [3] Aschemann H, Schindele D. Comparison of model-based approaches to the compensation of hysteresis in the force characteristic of pneumatic muscles. *IEEE Trans Ind Electron* 2014;61(7):3620–9.
- [4] Minh TV, Tjahjowidodo T, Ramon H, et al. Cascade position control of a single pneumatic artificial muscle–mass system with hysteresis compensation. *Mechatronics* 2010;20(3):402–14.
- [5] Harrison RG. A physical model of spin ferromagnetism. *IEEE Trans Magn* 2003;39(2):950–60.
- [6] Hassani V, Tjahjowidodo T, Do TN. A survey on hysteresis modeling, identification and control. *Mech Syst Sig Process* 2014;49(1–2):209–33.
- [7] Tan XB, Baras JS. Adaptive identification and control of hysteresis in smart materials. *IEEE Trans Autom Control* 2005;50(6):827–39.
- [8] Zhou M, He S, Hu B, et al. Modified KP model for hysteresis of magnetic shape memory alloy actuator. *IETE Tech Rev* 2014;32(1):29–36.
- [9] Xie SL, Mei JP, Liu HT, et al. Motion control of pneumatic muscle actuator using fast switching valve. *Proceedings of ASIAN MMS 2016 & CCMMMS 2016*. 2017. p. 1439–51.
- [10] Vo-Minh T, Tjahjowidodo T, Ramon H, et al. A new approach to modeling hysteresis in a pneumatic artificial muscle using the Maxwell-slip model. *IEEE/ASME Trans Mechatron* 2011;16(1):177–86.
- [11] Yeh TJ, Wu MJ, Lu TJ, et al. Control of McKibben pneumatic muscles for a power-assist, lower-limb orthosis. *Mechatronics* 2010;20(6):686–97.
- [12] Lin CJ, Lin CR, Yu SK, et al. Hysteresis modeling and tracking control for a dual pneumatic artificial muscle system using Prandtl–Ishlinskii model. *Mechatronics* 2015;28:35–45.
- [13] Bastien J, Michon G, Manin L, et al. An analysis of the modified Dahl and Masing models: application to a belt tensioner. *J Sound Vib* 2007;302(4):841–64.
- [14] Swevers J, Al-Bender F, Gansman CG, et al. An integrated friction model structure with improved presliding behavior for accurate friction compensation. *IEEE Trans Autom Control* 2000;45(4):675–86.
- [15] Oh JH, Bernstein DS. Semilinear Duhem model for rate-independent and rate-dependent hysteresis. *IEEE Trans Autom Control* 2005;50(5):631–45.
- [16] Lin CJ, Lin PT. Tracking control of a biaxial piezo-actuated positioning stage using generalized Duhem model. *Comput Math Appl* 2012;64(5):766–87.
- [17] Ismail M, Ikhouane F, Rodellar J. The hysteresis Bouc-Wen model, a survey. *Arch Comput Methods Eng* 2009;16(2):161–88.
- [18] Kiureghian AD, Song J. Generalized Bouc-Wen model for highly asymmetric hysteresis. *J Eng Mech* 2006;132(6):610–8.
- [19] Kuhnen K, Janocha H. Inverse feedforward controller for complex hysteresis nonlinearities in smart-material systems. *Control Intell Syst* 2001;29(3):74–83.
- [20] Zhang J, Merced E, Sepúlveda N, et al. Optimal compression of generalized Prandtl–Ishlinskii hysteresis models. *Automatica* 2015;57(C):170–9.
- [21] Kuhnen K. Modeling, identification and compensation of complex hysteretic nonlinearities: a modified Prandtl–Ishlinskii approach. *Eur J Control* 2003;9(4):407–18.
- [22] Zhang J, Merced E, Sepulveda N, et al. Inversion of an extended generalized

- Prandtl-Ishlinskii hysteresis model: theory and experimental results. Proceedings of American Control Conference (ACC), 2014. 2014. p. 4765–70.
- [23] Gu GY, Yang MJ, Zhu LM. Real-time inverse hysteresis compensation of piezoelectric actuators with a modified Prandtl-Ishlinskii model. *Rev Sci Instrum* 2012;83(6):65–83.
- [24] Wei TA, Khosla PK, Riviere CN. Feedforward controller with inverse rate-dependent model for piezoelectric actuators in trajectory-tracking applications. *IEEE/ASME Trans Mechatron* 2007;12(2):134–42.
- [25] Al Janaideh M, Mao J, Rakheja S, et al. Generalized Prandtl-Ishlinskii hysteresis model: hysteresis modeling and its inverse for compensation in smart actuators. 47th IEEE Conference on Decision and Control. 2008. p. 5182–7.
- [26] Janaideh MA, Rakheja S, Su CY. A generalized Prandtl-Ishlinskii model for characterizing the hysteresis and saturation nonlinearities of smart actuators. *Smart Mater Struct* 2009;18(4):045001.
- [27] Janaideh MA, Rakheja S, Su CY. An Analytical generalized Prandtl-Ishlinskii model inversion for hysteresis compensation in micropositioning control. *IEEE/ASME Trans Mechatron* 2011;16(4):734–44.
- [28] Jiang H, Ji H, Qiu J, et al. A modified Prandtl-Ishlinskii model for modeling asymmetric hysteresis of piezoelectric actuators. *IEEE Trans Ultrason Ferroelectr Freq Control* 2010;57(5):1200–10.
- [29] Zhang J, Merced E, Sepúlveda N, et al. Modeling and inverse compensation of hysteresis in vanadium dioxide using an extended generalized Prandtl-Ishlinskii model. *Smart Mater Struct* 2014;23(12):125017.
- [30] Gu GY, Zhu LM, Su CY. Modeling and compensation of asymmetric hysteresis nonlinearity for piezoceramic actuators with a modified Prandtl-Ishlinskii model. *IEEE Trans Ind Electron* 2014;61(3):1583–95.
- [31] Visintin A. *Differential models of hysteresis*. Berlin, Germany: Springer-Verlag; 1994.
- [32] Liu S, Su CY. A note on the properties of a generalized Prandtl-Ishlinskii model. *Smart Mater Struct* 2011;20(8):087003.
- [33] Yang MJ, Gu GY, Zhu LM. Parameter identification of the generalized Prandtl-Ishlinskii model for piezoelectric actuators using modified particle swarm optimization. *Sens Actuators A* 2013;189(2):254–65.
- [34] Landini G. Hysteresis identification and compensation using a genetic algorithm with adaptive search space. *Mechatronics* 2007;17(7):391–402.
- [35] Hansen N. The CMA evolution strategy: a comparing review. *Stud Fuzziness Soft Comput* 2006;192:75–102.
- [36] Wang Y, Handroos H, Carbone G. Modified Levenberg–Marquardt algorithm for backpropagation neural network training in dynamic model identification of mechanical systems. *J Dyn Syst Meas Control* 2017;139:1–14.



Sheng-Long Xie received both Bachelor and Master degrees in mechanical engineering from Anhui University of Technology, Ma'anshan, China in 2011 and 2014 respectively. He is currently a Ph.D. student at Key Laboratory of Mechanism Theory and Equipment Design of Ministry of Education, Tianjin University, China. His research interests include dynamics of parallel mechanisms and motion control of pneumatic servo systems.



Hai-Tao Liu received B.S., M.S., and Ph.D. in Mechanical Engineering from Tianjin University, Tianjin, China, in 2004, 2007, and 2010, respectively. From 2013 to 2014, he stayed at the Chair of Mechanics and Robotics at University of Duisburg-Essen with a fellowship from the Alexander von Humboldt (AvH) Foundation of Germany. Currently he is professor in School of Mechanical Engineering, Tianjin University. His research interests include robotics, kinematics and dynamics of parallel mechanisms, Lie group and Lie algebra, screw theory.



Jiang-Ping Mei received his Ph.D. degree from Tianjin University, Tianjin, China, in 2002. He is currently an associate professor and a Ph.D. candidate supervisor at Key Laboratory of Mechanism Theory and Equipment Design of Ministry of Education, Tianjin University, China. His research interests include manufacturing systems and industrial robots.



Guo-Ying Gu received the B.E. degree in electronic engineering and the Ph.D. degree in mechanical engineering from Shanghai Jiao Tong University, Shanghai, China, in 2006 and 2012, respectively. He is currently a Postdoctoral Research Fellow with the School of Mechanical and Power Engineering, Shanghai Jiao Tong University. He was a Visiting Researcher with Concordia University, Montreal, QC, Canada (from October 2010 to March 2011 and from November 2011 to March 2012). His research interests include motion control of nanopositioning stages for scanning probe microscopy applications, robust control, modeling, and control of smart material-based actuators with hysteresis.